Incommensurate superlattices in the Pb-substituted Bi-Sr-Ca-Cu-O superconductors

C. H. Chen, D. J. Werder, G. P. Espinosa, and A. S. Cooper
AT&T Bell Laboratories, Murray Hill, New Jersey 07974
(Received 31 October 1988)

We have studied incommensurate superlattice modulations in the Pb-substituted Bi-Sr-Ca-Cu-O single-crystalline superconductors by electron diffraction and electron microscopy. New incommensurate superlattice modulations characterized by a wave vector $Q=(0,1/p,0)$ (with $p>6$) have been observed. The incommensurate modulation arises from chemical substitutions with a sizable lattice displacive distortion.

Substitution of Pb into Bi-Sr-Ca-Cu-O superconductors has been found to increase the superconducting transition temperature.[1] However, the effect of Pb substitution on the microstructure of the crystal in regard to defect structure and superlattice modulation is still largely unknown. It is now well established that the 2:2:1:2 phase of the Bi-Sr-Ca-Cu-O superconductor exhibits a superlattice modulation which can be characterized by a wave vector $Q=(0,\frac{1}{4.76},1)$.[2,3] In earlier diffraction studies, some discrepancies existed between the results obtained by electron and x-ray diffraction. In particular, x-ray diffraction[1] showed incommensurate superlattice peaks located near $(0,\frac{1}{5},0)$ and $(0,\frac{2}{5},0)$ positions. Electron diffraction studies,[2-6] on the other hand, have revealed no superlattice peaks near $(0,\frac{1}{5},0)$. It is believed that the high density of planar stacking faults along the c axis can account for this discrepancy. Electron diffraction studies usually were performed from a much smaller area of the sample than the x-ray studies, so the highly defective areas could be avoided. Nevertheless, electron diffraction can also be complicated by the presence of double reflection and stacking faults which can cause forbidden reflections when viewed along some specific crystallographic directions. Interpretation of electron diffraction patterns along the [001] zone axis, therefore, could become very difficult and unreliable.

In this Brief Report, we report studies of the superlattice modulations observed in the single crystalline Pb-doped 2:2:1:2 Bi-Sr-Ca-Cu-O superconductors. New superlattice reflections are found which may help in understanding the cause (i.e., substitutional versus displacive) of the modulated structure. We address the substitutional-displacive issue for the origin of the superstructure.

Single crystals of the pure and Pb-substituted 2:2:1:2 phase were prepared by the flux method. The pure 2:2:1:2 crystals exhibit a $T_c(R=0)\sim 75$ K. Two Pb-substituted samples were prepared. One with a nominal starting melt composition (in mol%) of Bi_2O_3, 9.09; $SrCO_3$, 21.82; $CaCO_3$, 21.82; CuO, 43.64; and PbO, 3.63; and the other higher-Pb sample with Bi_2O_3, 17.74; $SrCO_3$, 25.16; $CaCO_3$, 12.90; CuO, 28.06; and PbO, 16.13. The metallic ratio of [Pb]/[Bi+Sr] for the low-Pb and the high-Pb samples is 0.081 and 0.266, respectively. The low-Pb sample showed an improved $T_c(R=0)\sim 85$ K whereas the high-Pb sample exhibited a $T_c(R=0)\sim 27$ K. Both plan-view and cross-sectional samples have been examined. Plan-view samples with c axis perpendicular to the foil surface were prepared by cleaving with adhesive tape and cross-sectional samples with a axis perpendicular to foil surface were prepared by mechanical polishing and ion milling. A JEOL 2000FX electron microscope operated at 200 kV was used in the present study.

Convergent beam electron diffraction patterns obtained from the Pb-substituted samples did not reveal any structural symmetry changes from the pure 2:2:1:2 phase. They all show a point group symmetry of *mmm*. Real-space examination of the pure and the Pb-substituted samples, however, showed significant differences in the crystal defect density. The low-Pb sample, which exhibited a higher T_c, was found to be the least defective and the high-Pb sample, on the other hand, exhibited a much lower T_c, and is highly defective with complicated defect structures. The most prominent defect observed in the high-Pb sample, as shown in Fig. 1, is the presence of striped domains with typical longitudinal and transverse dimensions ~ 1 and 0.1 μm, respectively. Two nonorthogonal striped domains can be seen, one is parallel to the $[1\bar{1}0]$ direction and the other is close to the [210] direction. There are other defects that occur in a much smaller scale ($\lesssim 50$ Å). The detailed nature of all these defects is not clearly known at present and further studies are now in progress. However, we suspect that the low-T_c ob-

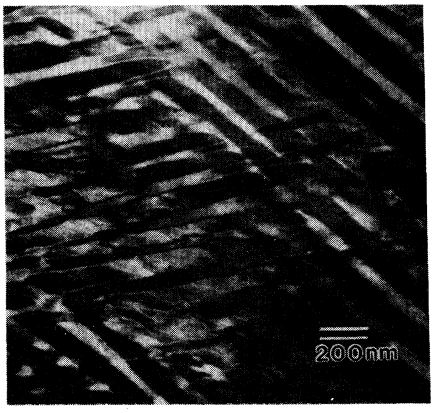

FIG. 1. Bright-field image showing the striped domains observed in the high-Pb sample.

served in the high-Pb sample could be related to the high-defect density present in the sample.

We present first the diffraction results obtained from the plan view samples (c axis perpendicular to the foil). In Fig. 2 selected area electron diffraction patterns along the [001] zone axes of the pure, low-Pb, and high-Pb samples are reproduced for comparison. Figure 2(a) for the pure 2:2:1:2 phase is identical to those obtained from a single grain in a polycrystalline 2:2:1:2 sample. Close examination of the diffraction patterns shown in Fig. 2 reveals clearly the differences due to Pb substitution. However, quantification of the differences in Fig. 2 caused by the presence of Pb appears to be difficult because of some complications due to electron diffraction effects, as mentioned above, that occur along the [001] zone axis. Specifically, the major problems we encounter in this case are as follows: First, the large lattice parameter along the c axis (i.e., parallel to the incident electron beam) would increase the probability of multiple scattering involving diffraction spots in the higher-order Laue zones; second, the ubiquity of stacking faults of the perovskite layers along the c axis would give rise to diffraction peaks which are normally forbidden in perfect crystals. Hence, we should not interpret all the extra spots in Fig. 2 as being caused by the superstructure.

Being aware of this complication of the electron diffraction patterns along the [001] zone axis, we have concentrated our studies on the cross-sectional samples with the [100] axis perpendicular to the thin-foil surface. With the thin-film sample now oriented with the [100] zone axis parallel to the electron beam, the above-mentioned diffraction complications are greatly reduced since the planar stacking faults along the c axis are now parallel to the electron beam and the lattice parameter along the incident electron-beam direction is much smaller ($a_0 = 5.4$ Å), reducing the probability of multiple reflections from the higher-order Laue zones.

Selected area electron diffraction patterns of the [100] zone axis for the pure, low-Pb and high-Pb single-crystalline samples are shown in Figs. 3(a), 3(b), and 3(c), respectively. For clarity, Fig. 3 is also illustrated schematically in Fig. 4. The superlattice reflections for the pure 2:2:1:2 phase shown in Fig. 3(a) are identical to those observed in the polycrystalline ceramics, and the superlattice modulation can be characterized by a reduced wave vector $Q_1 = (0, \frac{1}{4.76}, 1)$.[2,3] The appearance of the commensurate component of Q_1 along the c axis indicates that no superlattice spots are expected in a $(0,k,0)$ scan (i.e., along the b axis). In comparison with the pure 2:2:1:2 sample, the low-Pb sample [Fig. 3(b)] exhibits a new set of modulation superlattices characterized by a new wave vector $Q_2 = (0, \frac{1}{6.6}, 0)$, in addition to the Q_1-type superlattice observed in the pure sample. However, in this case the modulation wave vector $Q_1 = (0, \frac{1}{4.52}, 1)$. It still has a commensurate component along c, but the incommensurate modulation periodicity has now changed from $4.76b$ in the pure sample to $4.52b$. We note that the new superlattice wave vector Q_2 exhibits an incommensurate modulation ($6.6 \times b$) purely along the b axis without any component along c. Figure 3(b) also suggests that the Q_1-type superlattice reflection is broader in the low-Pb sample than the pure sample implying a shorter (< 200-Å) coherence length for this modulation. The new modulation superlattice Q_2, on the other hand, is quite sharp. For the high-Pb sample, it also shows two types of modulation superlattices similar to the low-Pb sample. However, the Q_2-type superlattice is now even broader and the incommensurate periodicity is now $7.52 \times b$ and $Q_1 = (0, \frac{1}{4.52}, 1)$ is identical to that observed in the low-Pb sample.

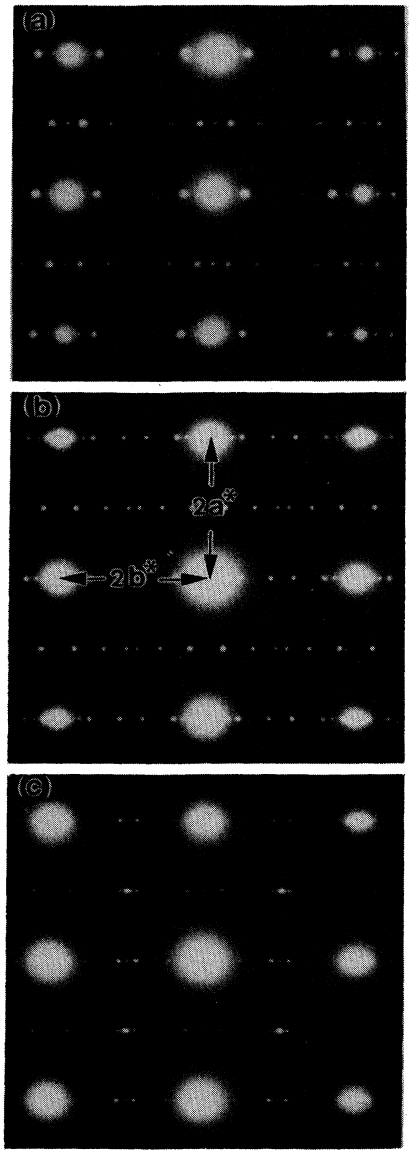

FIG. 2. Electron diffraction patterns along the [001] zone axes of the (a) pure, (b) low-Pb, and (c) high-Pb 2:2:1:2 samples. (a), (b), and (c) are reproduced with the same camera length.

There is increasing evidence suggesting that the presence of the incommensurate superlattice in the Bi-base superconductors originates primarily from the double Bi_2O_2 layers. The superlattice reflections could arise from substitutional and/or displacive modulations. The substitu-

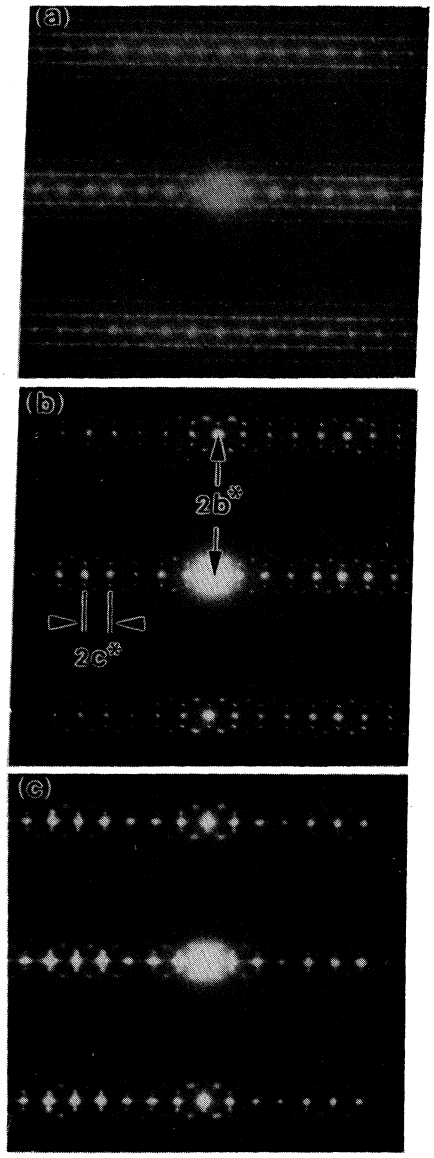

FIG. 3. Electron diffraction patterns along the [100] zone axis obtained from the (a) pure, (b) low-Pb, and (c) high-Pb samples. Note the presence of a new type of incommensurate superlattice reflections along b^* directly above (or below) the main lattice reflections. Some camera length is used for all diffraction patterns.

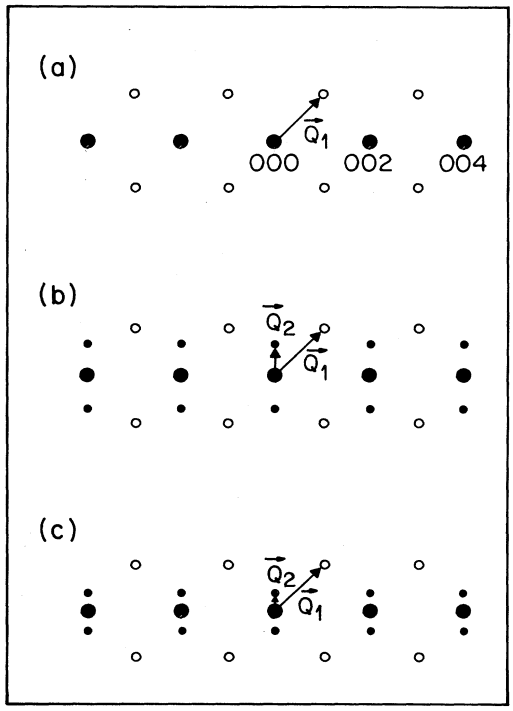

FIG. 4. Schematic illustrations of diffraction patterns shown in Figs. 3(a)–3(c). Diffraction spots due to the main sublattice, Q_1-type superlattice, and Q_2-type superlattice are represented by large filled circles, small open circles, and small filled circles, respectively.

tion of Sr or Ca for Bi and its associated distortion has been proposed[3,7] to explain the origin of the incommensurate modulation. A recent x-ray diffraction study[8] of the incommensurate modulation reported substantial displacive distortion of the Bi and Sr atoms and a sizable Cu atom displacement along the c axis. This is consistent with high-resolution electron microscopic lattice images[7] which also indicate large lattice distortions. The question of substitutional versus displacive modulation[8] has been an issue of some controversy in the Bi-based superconductors. We would like to point out here that a modulation that is caused by a chemical substitution can also give rise to a displacive distortion. A lattice displacive distortion in most cases is a consequence of more profound origins such as electronic or chemical instabilities. Our studies of the modulation superlattices in the Pb-substituted systems appear to suggest that the origin of the incommensurate modulation is due to chemical substitution. Based upon the analogy with the Ba-Bi-Pb-O system,[9] it is generally believed that Pb is substituting on the Bi sites. We mentioned earlier that the spatial coherence length and the intensity of the Q_1-type incommensurate modulation superlattice decreases with the amount of Pb substitution, this implies that Pb substitution occurs somewhat irregularly in the Bi lattice. This observation is also consistent with the idea that the incommensurate modulation in the Bi-based superconductors arises from chemical substitution.[1] What is unusual about the incommensurate modulation in this case is the abnormally large (up to 0.4 Å) (Ref. 8) displacive distortion. In the case of electronically driven incommensurate modulations (such as charge-density waves), a typical displacive distortion is $\sim$0.1 Å.[10] The unusually large displacive distortion associated with the incommensurate modulation in Bi-based superconductors makes the incommensurate superlattice reflections relatively insensitive to temperature. In fact, we have observed the superlattice spots for the pure 2:2:1:2 sample over a wide range of temperature from 30–1000 K, and have found no significant changes of the superlattice in-

tensities or widths. In this temperature range, we have also not observed any change in the superlattice wave vector within the accuracy of our measurement (~2%). The weaker superlattice intensity observed in the Pb-substituted samples suggests a smaller displacive distortion in comparison with the pure unsubstituted samples. In the pure samples, intergrowth of perovskite layers which contain one, two, and three Cu-O layers are commonly observed. As a result, diffuse streaking along the c axis is often observed in diffraction patterns as is shown in Fig. 3(a). One of the apparent effects of Pb substitution is to minimize the intergrowth problem, which significantly reduces the diffuse streaking as is shown in Figs. 3(b) and 3(c).

It appears that the most significant difference between the two sets of incommensurate superlattices shown in Figs. 3(a) and 3(b) is the appearance of a c^* component in the wave vector $Q_1=(0,\frac{1}{4.52},1)$. The presence of the c^* component suggests that the substitutional ordering is 180° out of phase from one Bi_2O_2 double layer to the next double layer. Our high-resolution lattice images obtained from undoped samples have shown that the Bi distribution in the Bi_2O_2 double layer was not homogeneous, and broke into Bi-rich and Bi-deficient bands in agreement with the observation made by Matsui, Maeda, Tanaka, and Horiuchi.[7] Lattice contractions and expansions along the b direction have been observed in the Bi-rich and Bi-deficient bands, respectively.[7] The Bi-deficient bands are believed to be due to Sr substitution of Bi. The out-of phase stacking of these Bi-rich or Bi-deficient layers along the c axis give rise to the c^* component of the Q_1-modulated superlattice. The Bi-rich and Bi-deficient bands were found to occupy seven and three lattice planes along b, respectively.[7] The separation of each lattice plane along b is 2.7 Å. For the Pb-substituted samples, we have also observed similar Q_1 modulation of the Bi-rich and Bi-deficient bands in the lattice images. However, due to the weaker Q_1-superlattice reflections in this case, details of the modulation were not as clearly resolved.

As shown in Fig. 3, the periodicity of the Q_2-incommensurate modulations changes with the amount of Pb substitution. Our lattice images suggest that the Q_2 modulation is spatially separated from the Q_1 modulation, although the coexistence of both types of modulation can sometimes be seen in a small region near their boundaries. Furthermore, our lattice images also indicate that the Q_2-modulated Bi layers stack in phase along the c axis, in contrast with the out-of-phase stacking observed for the Q_1 modulation. The in-phase stacking along the c axis is consistent with the absence of a c^* component observed in the diffraction studies [see Figs. 3(b) and 3(c)].

In conclusion, we have found that Pb substitution in the Bi-based superconductors gives rise to new additional incommensurate superlattice modulations without the presence of a c^* component. The new incommensurate superlattice modulation can be understood in terms of in-phase stacking of the Pb-substituted Bi double layers. Our studies suggest that the incommensurate modulation in the Bi-based superconductors is due to chemical substitutions which, in turn, give rise to a sizable displacive lattice distortion.

[1]S. A. Sunshine, T. Siegrist, L. F. Schneemeyer, D. W. Murphy, R. J. Cava, B. Batlogg, R. B. van Dover, R. M. Fleming, S. H. Glarum, S. Nahahara, R. Farrow, J. J. Krajewski, S. M. Zahurak, J. V. Waszczak, J. H. Marshall, P. Marsh, L. W. Rupp, Jr., and W. F. Peck, Phys. Rev. B **38**, 893 (1988).

[2]C. H. Chen, D. J. Werder, S. H. Liou, H. S. Chen, and M. Hong, Phys. Rev. B **37**, 9834 (1988).

[3]J. D. FitzGerald, R. L. Withers, J. G. Thompson, L. R. Wallenberg, J. S. Anderson, and B. G. Hyde, Phys. Rev. Lett. **60**, 2797 (1988); R. L. Withers, J. S. Anderson, B. G. Hyde, J. G. Thompson, L. R. Wallenberg, J. D. FitzGerald, and A. M. Stewart (unpublished).

[4]Y. Matsui, H. Maeda, Y. Tanaka, and S. Horiuchi, Jpn. J. Appl. Phys. **27**, L361 (1988).

[5]H. W. Zandbergen, P. Groen, G. van Tendeloo, J. van Landuyt, and S. Amelinckx, Solid State Commun. **66**, 397 (1988).

[6]T. M. Shaw, S. A. Shivashankar, S. J. La Place, J. J. Cumo, T. R. McGuire, R. A. Roy, K. H. Kelleher, and D. S. Yee, Phys. Rev. B **37**, 9856 (1988).

[7]Y. Matsui, H. Maeda, Y. Tanaka, and S. Horiuchi, Jpn. J. Appl. Phys. **27**, L372 (1988).

[8]Y. Gao, P. Lee, P. Coppens, M. A. Subramanian, and A. W. Sleight, Science **214**, 954 (1988).

[9]A. W. Sleight, J. L. Gillson, and P. E. Bierstedt, Solid State Commun. **17**, 27 (1975).

[10]J. A. Wilson, F. J. DiSalvo, and S. Mahajan, Adv. Phys. **24**, 117 (1975).

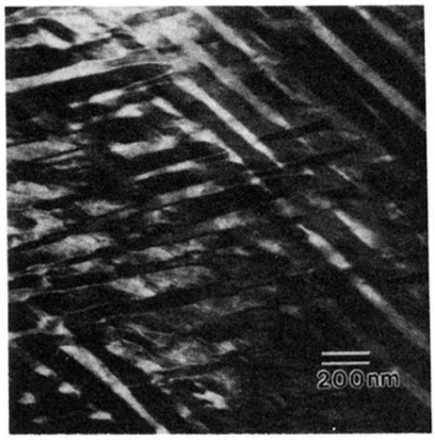

FIG. 1. Bright-field image showing the striped domains observed in the high-Pb sample.

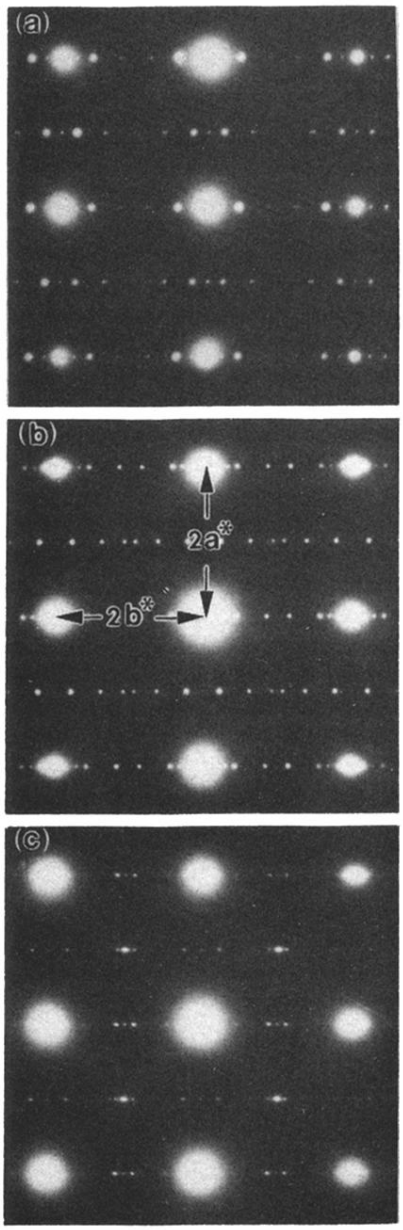

FIG. 2. Electron diffraction patterns along the [001] zone axes of the (a) pure, (b) low-Pb, and (c) high-Pb 2:2:1:2 samples. (a), (b), and (c) are reproduced with the same camera length.

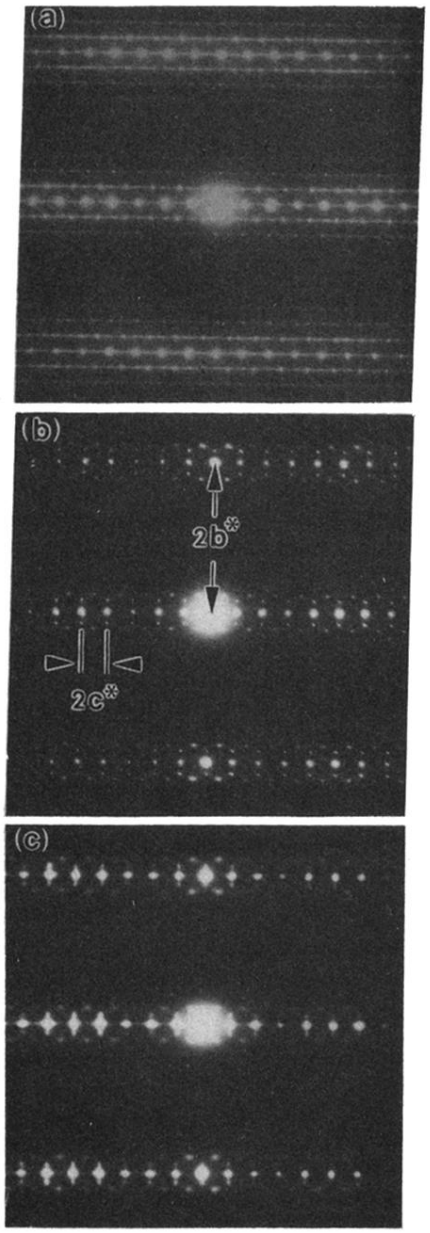

FIG. 3. Electron diffraction patterns along the [100] zone axis obtained from the (a) pure, (b) low-Pb, and (c) high-Pb samples. Note the presence of a new type of incommensurate superlattice reflections along b^* directly above (or below) the main lattice reflections. Some camera length is used for all diffraction patterns.